I. Supplemental Figures and Legends

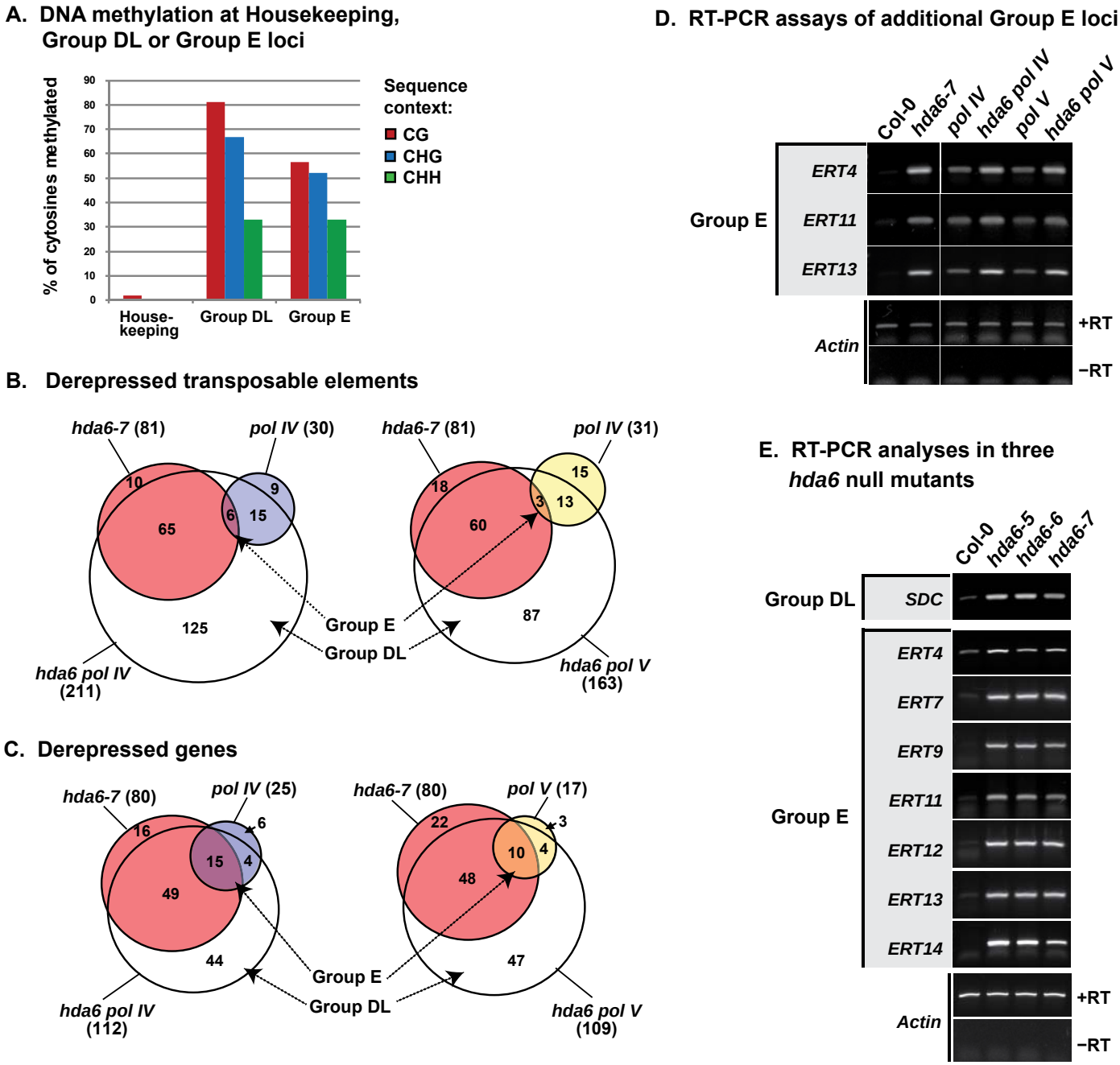

Figure S1, Related to Figure 1. Loci derepressed in *hda6*, pol IV or pol V mutants.

(A) DNA methylation at housekeeping genes, Group DL or Group E loci. Bar graphs show the percentage of CG, CHG or CHH sites that were >10% methylated in wild-type Col-0, at loci of three different expression groups: housekeeping genes, Group DL loci and Group E loci (see Table S1C for a list of loci in each group). The analysis was performed using genome-wide bisulfite sequencing data of Stroud et al., 2013.

(B and C) Venn diagrams showing derepressed TEs (C) and derepressed genes (D) as separate categories of derepressed loci (TEs and genes were grouped in Figure 1B of the main paper). In all Venn analyses, uniquely-mapped, polyA+ reads were used to evaluate derepression of loci by comparing total counts at each locus in the mutant relative to Col-0, with a minimum 4-fold increase in the mutant and p value < 0.01. All RNA-seq data were normalized to the total number of mapped reads in each sample.

(D and E) RT-PCR analyses of Group E loci and the Group DL locus, *SDC* in wild-type (Col-0) or the indicated mutant backgrounds. *Actin* serves as a loading control. Controls omitting reverse transcriptase (−RT) yielded no amplifications products, as shown for *Actin*.

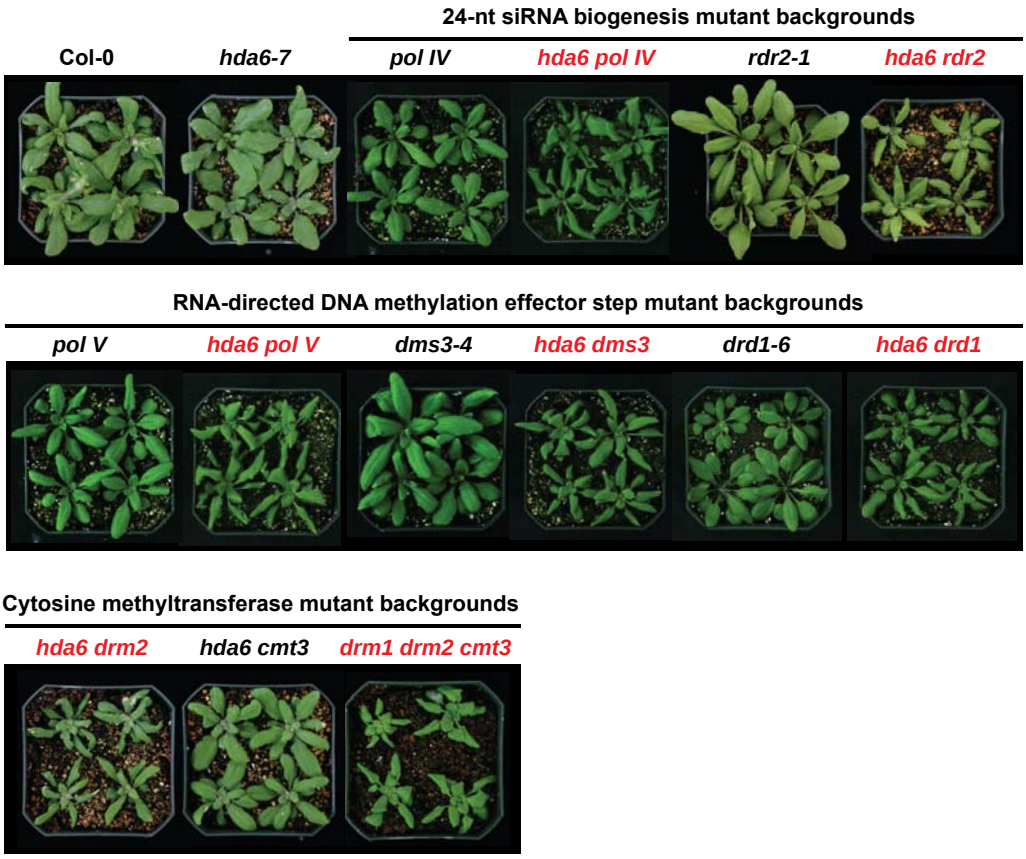

Figure S2, Related to Figure 2. The *SDC* overexpression phenotype occurs in double mutants pairing *hda6* with RdDM pathway mutants.

Images of 21-day-old *A.thaliana* plants are shown. Lines displaying the dwarfed and twisted phenotype associated with *SDC* gene overexpression are labeled in red; all are double mutants that harbor *hda6-7* in combination with mutations disrupting known components of the RdDM pathway, with the exception of the *drm1 drm2 cmt3* control. The HDA6-dependence of both CG and CHG maintenance methylation (Earley et al, 2010) may account for *cmt3* and *hda6* mutations being interchangeable for the *SDC*-dependent mutant phenotype given that CMT3 is the major CHG maintenance methyltransferase. This hypothesis is also consistent with the similar, partial derepression of SDC in *cmt3* or *hda6* mutants as shown in Figure S3B.

A. Chop-PCR DNA methylation assays

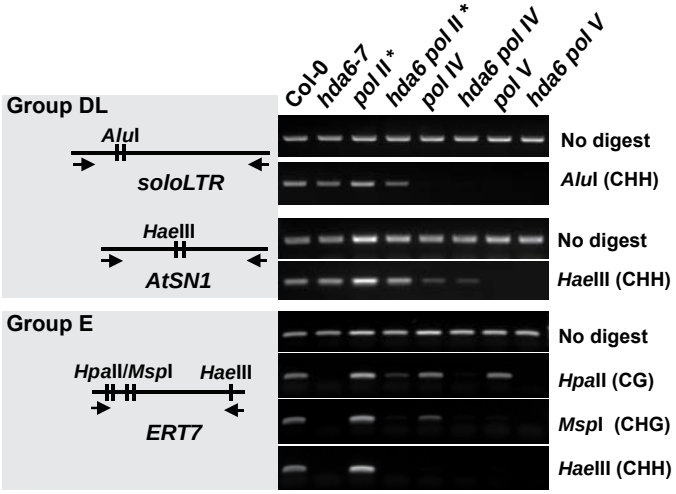

B. Effects of methyltransferase mutants on Group DL and Group E Loci

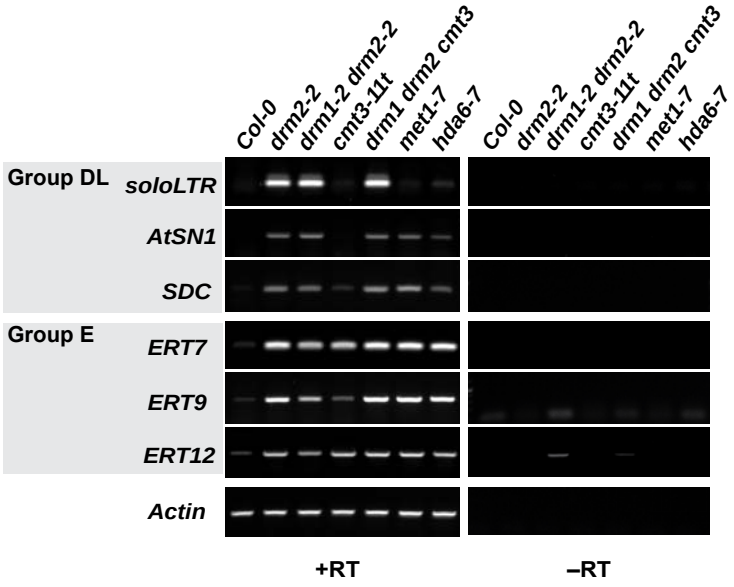

Figure S3, Related to Figure 3. Cytosine methylation and silencing of Group DL and Group E loci.

(A) DNA methylation at Group DL and Group E loci, assayed using methylation-sensitive restriction endonuclease digestion followed by PCR (Chop-PCR). Genomic DNA was digested with the indicated methylation-sensitive restriction endonucleases, and then amplified by PCR using primers that flank the endonuclease recognition sites (see diagrams at left). The different enzymes tested report on cytosine methylation in different sequence contexts: *Alu*I reports on CHH methylation at two sites in the *soloLTR* locus; *Hae*III reports on two CHH sites in the *AtSN1* locus; and in the *ERT7* locus, *Hpa*II tests CG, *Msp*I tests CHG and *Hae*III tests CHH methylation, where H represents any base other than G. Loss, or decrease, of a PCR product reflects a loss of methylation, such that the DNA is cut by the restriction endonuclease and PCR of the interval fails.

(B) Loss of silencing in cytosine methyltransferase mutants in comparison to *hda6-7*. RT-PCR was used to detect derepression of the indicated loci in mutants for the major cytosine methyltransferases. Actin serves as a loading control. Controls omitting reverse transcriptase (−RT) are at right.

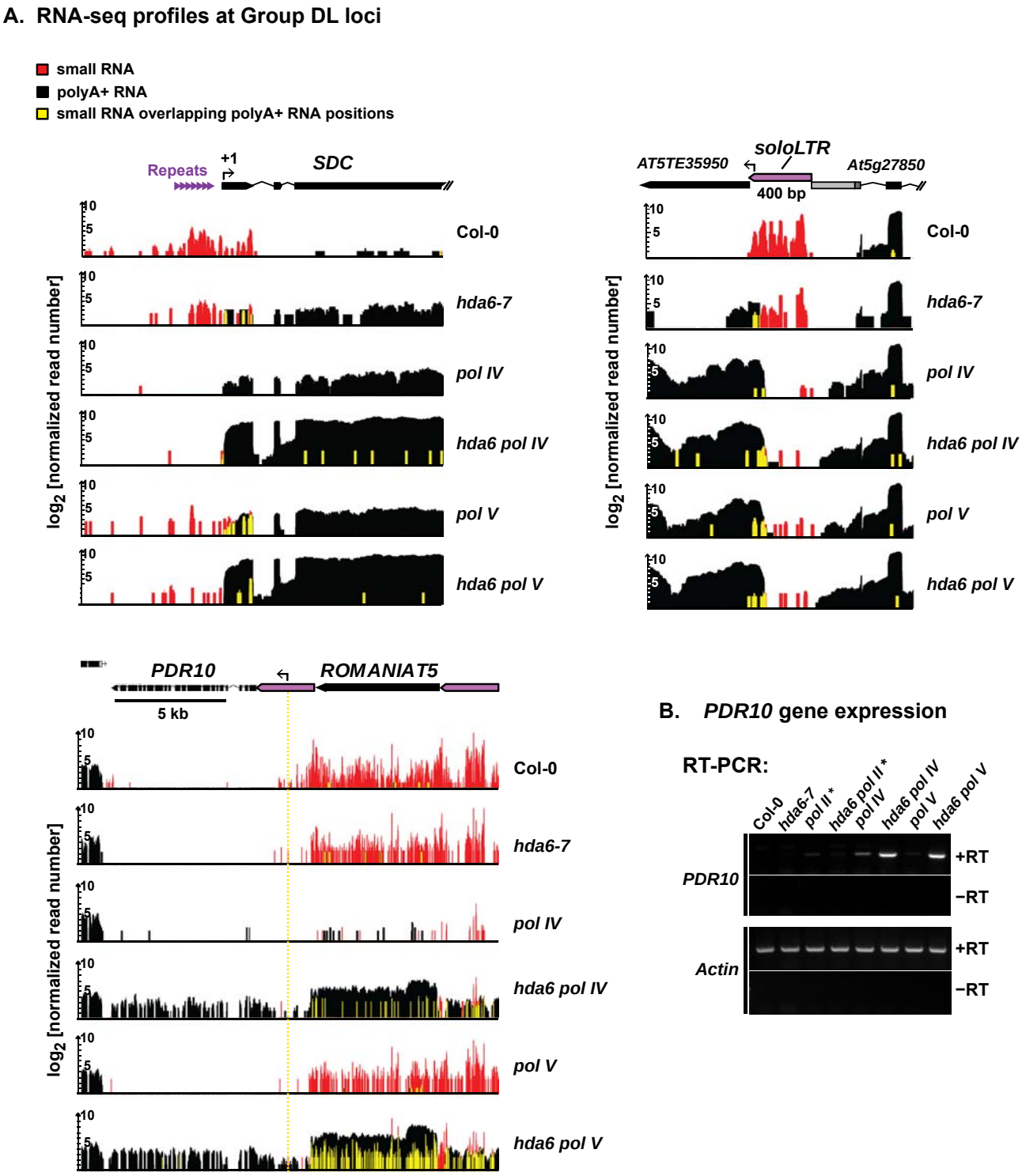

Figure S4, Related to Figure 4.

RNA-seq and RT-PCR analyses of Group DL locus derepression in *hda6* and/or pol IV/V mutants.

(A) RNA-seq profiles at Group DL loci. Data tracks show polyA+ RNA reads (black vertical bars), small RNA reads (red vertical bars) and overlapping read data (yellow vertical bars) detected in the following samples: Col-0, the single mutants: *hda6-7*, *pol IV* and *pol V*, and the double mutants: *hda6 pol IV* and *hda6 pol V*. Repetitive DNA elements (purple) situated upstream of polyA+ RNA transcription units are a source of Pol IV-dependent 24-nt siRNAs in wild-type plants (Col-0). The 3' long terminal repeat (purple) of *ROMANIAT5* overlaps the 5' untranslated region of a protein-coding gene, *PDR10*, whose silencing is double-locked by HDA6 and RdDM. Read counts are normalized by total mapped reads and shown in $\log_2$ units.

(B) *PDR10* gene expression was confirmed using conventional RT-PCR followed by agarose gel electrophoresis. Controls omitting reverse transcriptase (−RT) are shown below *PDR10* and the *Actin* (loading control) panels.

A. The RT-PCR assays of Figure 5B, with control reactions performed without reverse transcriptase (- RT) included

Mutant alleles used in this figure:

hda6-5	=	*axe1-4*, null for HDA6
hda6-6	=	*axe1-5*, null for HDA6
nrpd1	=	null for Pol IV largest subunit
nrpe1	=	null for Pol V largest subunit

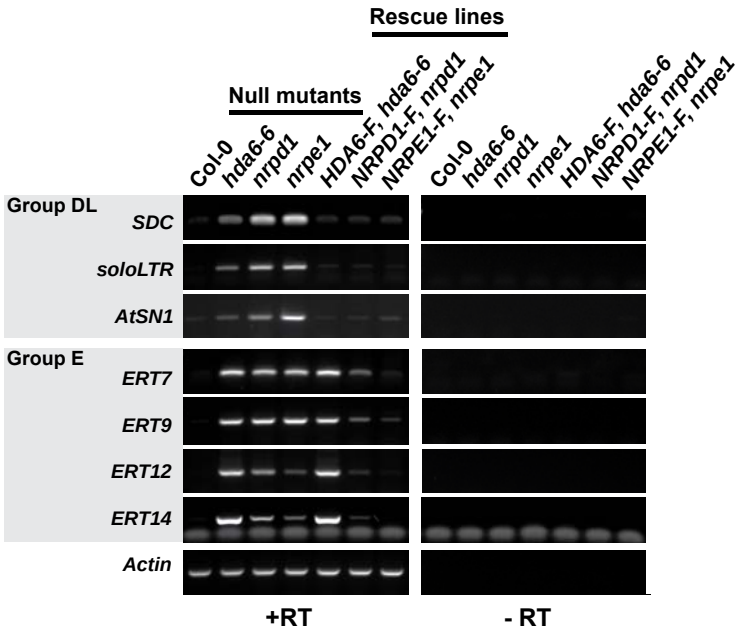

B. Analysis of lines expressing catalytically inactive HDA6 (RT-PCR)

Alignment of deacetylase active site residues

```
HDLP   159  FKRILYIDLDAHHCDGVQEAFYD  A.aeolicus
RPD3   177  HPRVLYIDIDVHHGDGVEEAFYT  S.cervisiae
HDAC1  167  HQRVLYIDIDIHHGDGVEEAFYT  H.sapiens
HDA19  175  HERVLYVDIDIHHGSGVEEAFYA  Arabidopsis
HDA6   179  FKRVLYIDIDVHHGDGVEEAFYT  Arabidopsis
            186 188 190
```

Mutated to Alanines in transgenic lines:

- HDA6-F (D186A)
- HDA6-F (D188A)
- HDA6-F (D190A)
- HDA6-F (all mutations)

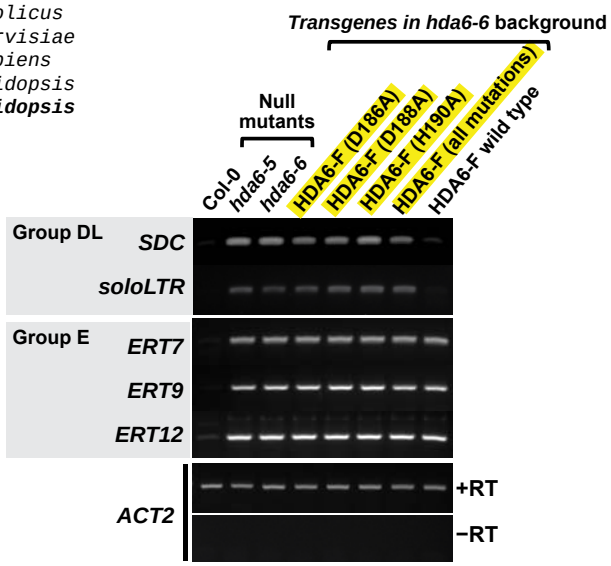

Figure S5, Controls for Figure 5 and assays indicating histone deacetylase activity of HDA6 is required for silencing Group DL loci.

(A) Complete version of the RT-PCR assay shown in Figure 5B, including control reactions omitting reverse transcriptase (RT). (B) Analysis of lines expressing catalytically inactive HDA6. Multiple alignment of amino acids in the active sites of the lysine deacetylases Aquifex HDLP, yeast Rpd3, human HDAC1 and *Arabidopsis* HDA6 and HDA19 (top left). The *hda6-6* null mutant was transformed with transgenes that express FLAG epitope-tagged HDA6 (HDA6-F) bearing alanine substitutions at the highlighted amino acids critical for HDA6 activity (D186A, D188A and D190A), or with a wild-type HDA6-F construct (see Earley et al. 2010). RT-PCR assays are shown for expression of Group DL and Group E in transgenic plants expressing the various forms of HDA6. Note that none of the active site mutants of HDA6 can rescue the *hda6-6* null mutation and re-establish silencing of the Group DL loci. By contrast, the wild-type version of the HDA6 transgene does rescue the mutant and restore silencing. At Group E loci, failure to restore silencing results from the loss of silent locus identity, which is not restored simply by restoring HDA6 activity.

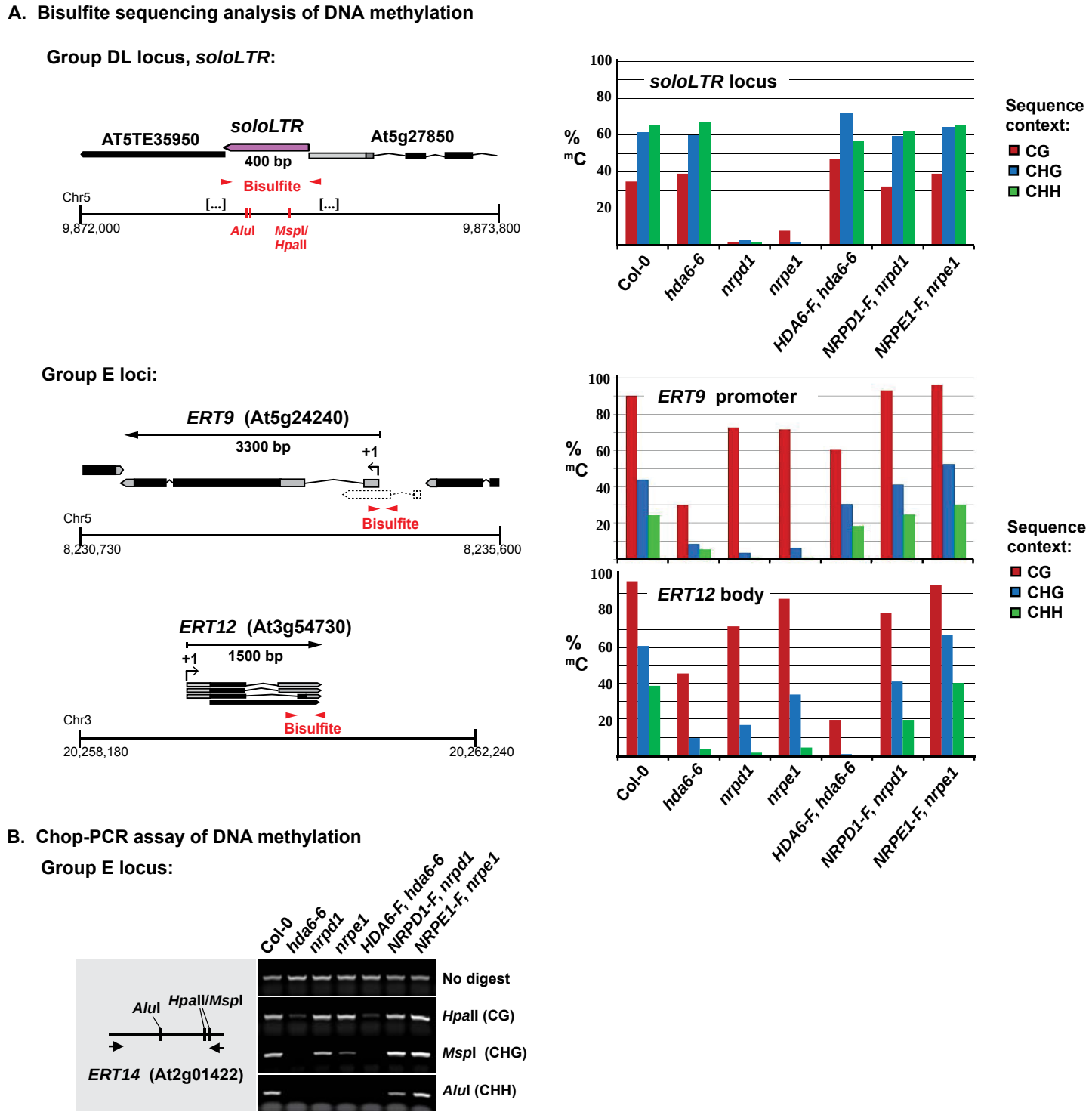

Figure S6, Related to Figure 5. DNA methylation assays at *soloLTR*, *ERT9*, *ERT12* and *ERT14* loci

(A) DNA methylation as determined by bisulfite sequencing. Genomic DNA from wild-type Col-0, the single mutants: *hda6-6*, *nrpd1* (*pol IV*) or *nrpe1* (*pol V*), and their respective transgenic rescue lines was subjected to bisulfite conversion. Strand-specific primers were then used to amplify DNA from the Group DL locus *soloLTR*, and from the Group E loci *ERT9* and *ERT12*; the PCR amplicons are indicated by red arrows in the gene diagrams. At least 30 independent clones were sequenced per PCR amplicon. The percentage of methylated cytosines in CG, CHG or CHH contexts (with H being a base other than G), is shown in the bar graphs.

(B) DNA methylation as determined Chop-PCR. Genomic DNA was digested with methylation-sensitive restriction endonucleases, then amplified by PCR using primers that flank endonuclease recognition sites in the *ERT14* locus. The different enzymes tested report on cytosine methylation in different sequence contexts: *Hpa*II tests CG, *Msp*I tests CHG and *Alu*I tests CHH methylation, where H represents any base other than G. Loss of a PCR product reflects a loss of methylation, such that the DNA is cut by the restriction endonuclease and PCR of the interval fails.

A. Effect of HDA6 rescue on 24-nt siRNA levels

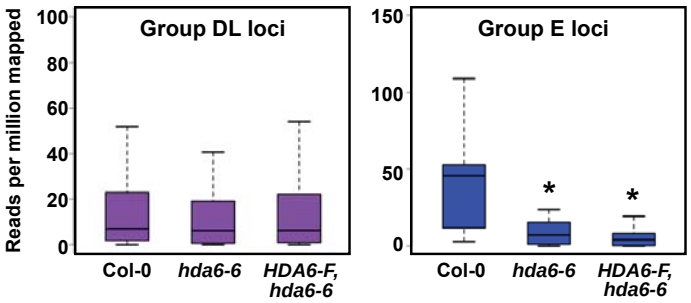

B. siRNA profiles at Group DL locus, *SDC*

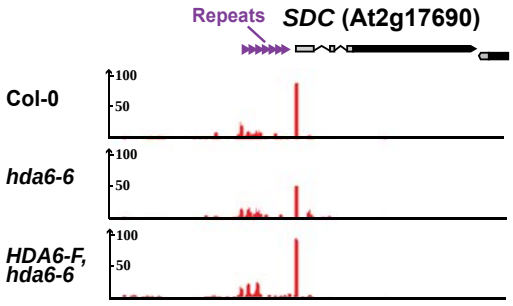

C. siRNA profiles at Group E loci

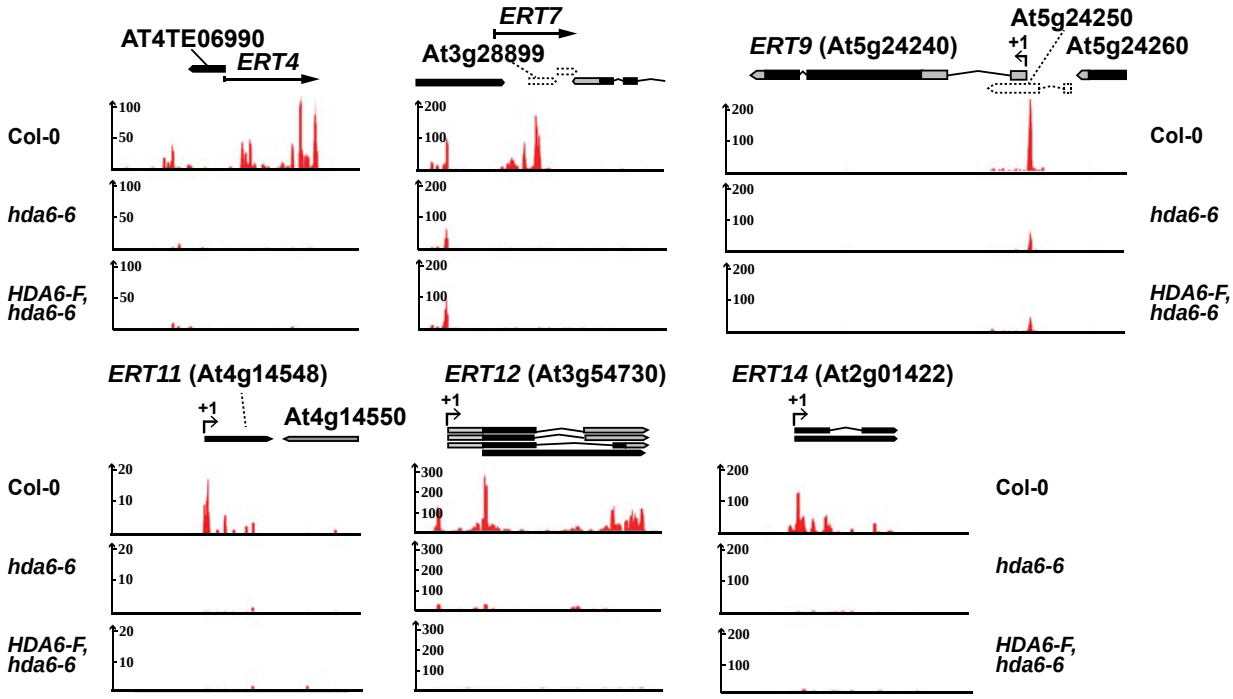

D. Wilcoxon rank sum tests for statistical significance

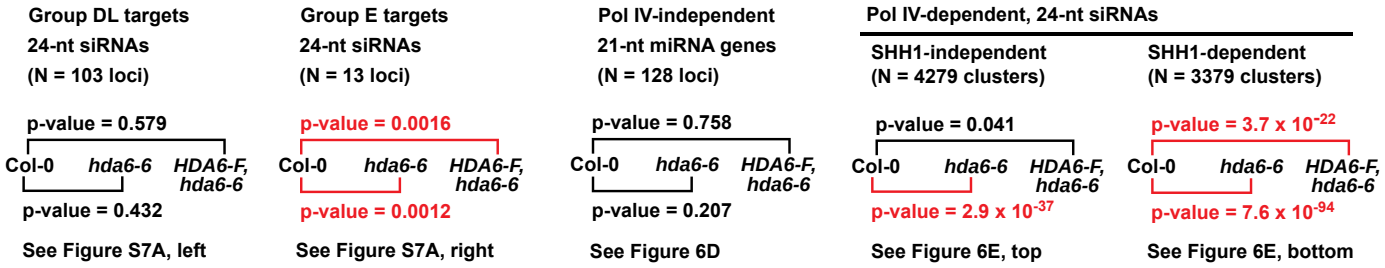

Figure S7, Related to Figure 6. Small RNA profiles and tests for changes in small RNA abundance at loci silenced by HDA6

(A) Boxplot analysis of the effects of HDA6 mutation and rescue on 24 nt siRNAs generated from Group DL (left panel) or Group E (right panel) loci. All read counts are normalized to total mapped read numbers. Asterisks above boxplots indicate significant reduction relative to Col-0 ($p < 0.002$, Wilcoxon rank-sum test).

(B and C) Small RNAs detected at representative Group DL and Group E loci in wild-type Col-0, *hda6-6* and *HDA6-F hda6-6* samples are depicted as red vertical bars. Values are normalized by total mapped reads.

(D) Statistical significance tests for data in Figures 6D, 6E and S7A. Small RNAs detected within functionally-defined clusters were tallied for each sample to obtain per-cluster small RNA abundances (in reads per million mapped). Wilcoxon rank-sum tests for significant shifts in the distribution of small RNA abundance yielded p-values indicated above and below the square brackets. Col-0 vs. mutant comparisons in which we can reject the null hypothesis that no change in small RNA abundance occurred, with $p<0.002$, are marked by asterisks in Figures 6E and S7A. The miRNA gene coordinates are defined in miRbase (Kozomara and Griffiths-Jones, 2011), and the 24-nt siRNA clusters and Pol IV/SHH1-dependencies are defined in (Law et al., 2013).

II. Supplemental Tables and Legends

Table S1, Related to Figure 1. Derepressed genes and transposons in mutants defective for HDA6, Pol IV or Pol IV, alone or in combination.

Gene or transposable element loci derepressed at least 4-fold (log-ratio > 2) in the specified mutant are listed (Worksheets A and B, respectively). Log-ratios are computed as the log base 2 ratio of the per-locus RPKM in the mutant relative to wild-type (Col-0) values. The formula for RPKM is $(10^9 \times C) / (N \times L)$, where C is the number of uniquely mapped reads at the locus, N is the total number of uniquely mapped reads in the sample and L is the length of the locus (Mortazavi et al., 2008). If no reads mapped to a locus (C = 0), then C is set to 0.5. P-values for differential expression in each mutant are estimated using a normal distribution with reference to the expected value in Col-0. Loci in the expression groups used for comparative analyses of Group DL, Group E and housekeeping gene loci are listed in Worksheet C**.**

Table S2, Related to Extended Experimental Procedures. Oligonucleotide primers used in the study.

The table shows the gene locus name, locus identifier, primer name, primer sequence and reference (where appropriate) for each oligonucleotide primer or TaqMan probe used in the study.

RT-PCR assays:

Target locus	AGI #	Primer name	Sequence (5' – 3')	Direction	Reference / Notes
SDC	At2g17690	SDC_RT_F (JP3395)	AATGTAAGTTGTAAACCATTTGAACGTGACC	Fwd	Johnson et al. 2008
		SDC_RT_R (JP3396)	CAGGCATCCGTAGAACTCATGAGC	Rev	
soloLTR	btwn AT5TE35950 & AT5G27850	soloLTR-A_F	ATCAATTATTATGTCATGTTAAAACCG	Fwd	Wierzbicki et al. 2008
		soloLTR-A_R	TGTTTCGAGTTTTATTCTCTCTAGTCT	Rev	
AtSN1	AT3TE63860	AtSN1_A-F	ACCAACGTGTTGTTGGCCCAGTGGTAAATC	Fwd	Herr et al. 2005;
		AtSN1_A-R	AAAATAAGTGGTGGTTGTACAAGC	Rev	Wierzbicki et al. 2008
PDR10	At3g30842	PDR10_F	TGGAATCATCTTTTGGAGCC	Fwd	Yokthongwattana et al. 2010
		PDR10_R	ACTCAACAACCGTCTCACCC	Rev	
ERT4	AT4TE06990 flanking	ERT4_nRT_F3	CAAAGTTTTCCCGACTTCATCCTTTGC	Fwd	this study
		ERT4_nRT_R3	CGCTTCTGTTACTTATTATCCAACCTG	Rev	
ERT7	At3g28899	ERT7_RT_F	GCCAATCTATCCAAGGCAGAGACG	Fwd	this study
		ERT7_RT_R	TTACACCACATCTGATCCCTTTACTCTACC	Rev	
ERT9	At5g24240	ERT9_RT_F2	CTTACTCCAATAGACCATGGCTATTGC	Fwd	this study
		ERT9_RT_R2	GGCTTCTGCATCATGTATGATTTGCTCG	Rev	
ERT11	At4g14548	ERT11_RT_F3	CAATAAAGTCTAAATCCTTTCATCTACGG	Fwd	this study
		ERT11_RT_R3	CTTCTTACCGTAAACGGCGGTGAG	Rev	
ERT12	At3g54730	ERT12_RT_F	CAGGCTTTGAGCCCTCTAGATCTGG	Fwd	this study
		ERT12_RT_R	ACTTCGGAGAGGTGTGGGGTTGC	Rev	
ERT13	At1g67105	ERT13_RT_F3	TAGACTACATCAAGATAGATGTAATCGGTGG	Fwd	this study
		ERT13_RT_R3	TATCCACGCGTCAGGAATCGAGC	Rev	
ERT14	At2g01422	ERT14_RT_F3	CCATTCGTGTTTAGGTTGAGTTAAGTGAGG	Fwd	this study
		ERT14_RT_R3	CACTGGAAATATAGATTTCATTGATAGAAGATCTG	Rev	
Actin7	At5g09810	Actin_RT_R	AAGTCATAACCATCGGAGCTG	Fwd	Earley et al. 2010
		Actin_RT_F	ACCAGATAAGACAAGACACAC	Rev	

Droplet Digital RT-PCR assays:

Target locus	Forward primer	Reverse primer	PrimeTime / TaqMan probe	
SDC	GCGGTTCCAGACATATCCTC	AACGCTCCAAATAGTTTGTATGC	AGTTGAACTCTCGTGCTCAAAGATCTGC	PrimeTime Std qPCR assay (IDT)
ERT7	CAATCTATCCAAGGCAGAGACG	GCATGGGTGGTGAGATAAAAC	CAAAGACCCGAAGGAGTGAGAGCC	PrimeTime Std qPCR assay (IDT)
ACT2	LifeTech TaqMan Gene Exp. Assay: At02329915_s1			ABI/LifeTech

Chop-PCR assays:

Target locus	AGI #	Primer name	Sequence (5' – 3')	Direction	Primer reference
soloLTR	btwn AT5TE35950 & AT5G27850	soloLTR-C_F	ATAAAACTCGAAACAAGAGTTTTCTTA	Fwd	Wierzbicki et al. 2008
		soloLTR-C_R	TAATGGTATTATTTTGATCAGTGTTAT	Rev	
AtSN1	AT3TE63860	AtSN1_A-F	ACCAACGTGTTGTTGGCCCAGTGGTAAATC	Fwd	Wierzbicki et al. 2008
		AtSN1_A-R	AAAATAAGTGGTGGTTGTACAAGC	Rev	
ERT7	At3g28899	ERT7_Chop_F4	CGCCGCCTGTATTTAGGGTTACC	Fwd	this study
		ERT7_Chop_R4	GGATAGAAACGTCTCTGCCTTGGATAG	Rev	
ERT14	At2g01422	ERT14_Chop_F1	GGACCGTTGAATTAATTACACACATTTATTCC	Fwd	this study
		ERT14_Chop_R1	CCGGTGCTGAGAAAGCCACC	Rev	

Bisulfite sequencing analyses:

Target locus	AGI #	Primer name	Sequence (5' – 3')	Direction	Primer reference
SDC	At2g17690	JP3551	TAAGTTTTATTATTTGGATTTAAAGYGGATAATATTA-TTTTAATYGAAAAAGTTGGAATGGGTTTGGAGAGTTT	Fwd	Henderson & Jacobsen 2008
		JP3552	AATCTCTAAAATTTTTTTATTTTACTCATTCTACTTT-AAACCTCTATCTTATAAATACACACAAACCCTAATAT-ATTTTATATTAAAA	Rev	
soloLTR	btwn AT5TE35950 & AT5G27850	soloLTR_bis_F2	GAYAAATAAATTTTTTATTYAAGTATATTAAGTGTA-GATTATTGTYTTYAG	Fwd	this study
		soloLTR_bis_R2	CTCRAAACAARARTTTTCTTATTRCTTTCTCTTTCTC	Rev	
ERT9	At5g24240	ERT9_bis_F1	GAATTTGGTAATTTYTAGATTYGTYTGATAAAAGATTTGYG	Fwd	this study
		ERT9_bis_R1	TCATCRAAACCRATACAATTCATCATCCATRATC	Rev	
ERT12	At3g54730	ERT12_bis_F1	GTTYATYGAGAAGTGGTGGTTTTYG	Fwd	this study
		ERT12_bis_R1	CACTTARATTTRTCCTCCCTATCTCTCAC	Rev	

qPCR for chromatin immunoprecipitation:

Target locus	AGI #	Primer name	Sequence (5' – 3')	Direction	Primer reference
SDC	At2g17690	SDC_ChIP_body1F	TGACCCTCCCAAAACGATAG	Fwd	this study
		SDC_ChIP_body1R	GAAACCGAGAAACAGGCATC	Rev	
SDC	At2g17690	SDC_ChIP_body2F	GCGTCAACAAGAACCATTCC	Fwd	this study
		SDC_ChIP_body2R	GTGTGACGCGAAAGAATGTG	Rev	
SDC	At2g17690	SDC_ChIP_UpstrF	TTACCACTTGGACCCAAAGC	Fwd	this study
		SDC_ChIP_UpstrR	AATAGGGTTGTTGGGCTCTC	Rev	
soloLTR	btwn AT5TE35950 & AT5G27850	soloLTR_ChIP_F (A142)	GGATAGAGATGAATGATGGATAATGACA	Fwd	Wierzbicki et al. 2008
		soloLTR_ChIP_R (A143)	TTATTTTGATCAGTGTTATAAACCGGATA	Rev	
ERT7	At3g28899	ERT7_ChIP_bodyF	CCAATCTATCCAAGGCAGAGAC	Fwd	this study
		ERT7_ChIP_bodyR	TTCAAAGACCCGAAGGAGTG	Rev	
ERT9	At5g24240	ERT9_ChIP_PromF	GGAAACGGTATCTGCCCTAC	Fwd	this study
		ERT9_ChIP_PromR	TGACCTCGCTGACTTTTGAC	Rev	

III. Extended Experimental Procedures

Genetic crosses and transgenic lines: Crosses were performed to obtain double mutants: *hda6-7 nrpb2-3, hda6-7 nrpd1-3, hda6-7 nrpd1-3*, *hda6-7 nrpe1-11*, *hda6-7 rdr2-1, hda6-7 drm2*, *hda6-7 cmt3-11t, hda6-7 dms3-4, hda6-7 drd1-6* and triple mutants: *hda6-7 drm2 cmt3*, *hda6-7 nrpd1-3 sdc, hda6-7 nrpe1-11 sdc. hda6-6* complemented by *302-gHDA6-FLAG* was described in Earley et al. (2010); *302-gNRPD1-FLAG nrpd1-3* and *302-gNRPE1-FLAG nrpe1-11* rescue lines were initially described in Pontes et al. (2006).

Chromatin Immunoprecipitation (ChIP): 3 g of 14-day-old rosette leaf tissue was cross-linked in 0.5% formaldehyde, frozen, and ground in 15 mL Honda buffer (0.44 M Sucrose, 1.25% Ficoll, 2.5% Dextran T40, 20 mM Hepes KOH, pH 7.4, 10 mM $MgCl_2$, 0.5% Triton X100, 5 mM DTT, 1 mM PMSF, 1% Plant Protease Inhibitor Cocktail (Sigma, IL, USA). The extract was subjected to centrifugation, the pellet was resuspended in 1mL Honda buffer, and then cleared by successive washing. The final nuclear pellet was suspended in 1 ml Nuclei Lysis buffer (50mM Tris-HCl, pH 8, 10mM EDTA, 1% SDS, 1mM PMSF, 1% Plant Protease Inhibitor Cocktail), and sonicated such that the average fragment size of DNA was ~500 bp. Chromatin aliquots were combined with 1 mL Dilution Buffer (1.1% Triton X100, 1.2mM EDTA, 167mM NaCl, 16.7 mM Tris-HCl, pH 8) and centrifuged 10 min at 16,000 x g. The supernatant was combined with 5 µL of antibody against H3K9/K14Ac (Millipore Cat # 06-599), H3K9me2 (Upstate Cat #07-441), or HDA6, and incubated at least 3 h at 4°C. 50 µl Protein G Dynabeads (Life Technologies, CA, USA) were added and the mixture incubated for 15 min at RT. Beads were washed five times with Binding/Washing buffer (150mM NaCl, 2mM EDTA, 1% Triton X100, 0.1% SDS, 1mM PMSF, 20mM Tris-HCl, pH 8) and twice with TE (1mM EDTA, 10mM Tris-HCl, pH 8). Cross-links were reversed by adding 100 µl of 10% Chelex (BioRad, CA, USA) to the beads and heating at 99°C for 10 min, then adding 20 µg Proteinase K and incubating at 43°C for 1 hr. Protease K was inactivated by heating to 95°C and samples were concentrated using a PCR purification column (Qiagen, MA, USA).

RNA sequencing procedures: For small RNA sequencing, 40 µg total RNA was subjected to 18% polyacrylamide gel electrophoresis. Gel slices were excised for the 15-45 nt size-range, then eluted for library preparation following recommendations of the Illumina Small RNA v1.5 Sample Preparation Guide, except that customized 5'-adapters replaced kit 5' adapters. Briefly, distinct 3' and 5' RNA-DNA hybrid adapters were ligated sequentially to the pool of small RNAs;

ligation products were reverse-transcribed and amplified by PCR. The 3' adapter (Illumina) is optimized for ligation to small RNAs with a 3' hydroxyl group (enzymatically cleaved). Each 5' adapter contained a unique 4-nt index. Final libraries were quantified using Quant-iT Picogreen dsDNA Reagent (Invitrogen). To remove excess adaptors, the library pool was excised from a 6% polyacrylamide gel. Templates were assessed by migration on a Bioanalyzer DNA1000 chip (Agilent). The library pool was sequenced to 75 cycles on an Illumina GAIIx using an Illumina v4 small RNA cluster generation kit and v4 reagents. For mRNA sequencing, total RNA preparations were enriched for polyadenylated RNA using DynaBeads Oligo(dT) (Invitrogen) and mRNA-Seq libraries were prepared according to Illumina, with indexed adaptors (Illumina Multiplex Sample Prep Oligos) added during amplification. The final library pool (mean modal size 295 bp) was cleaned of excess adaptors using Agencourt AMPure XP beads (Beckman Coulter Genomics) and quantified and assessed as above. An equimolar pool (18 ng/ul) was prepared and clustered on a single read flowcell. Sequencing was performed on an Illumina GAIIx instrument using a v2 cluster generation kit, v4 Sequencing reagents and SBS 2.8 instrument software, for 76 cycles + 7 index cycles.

Fasteris SA (http://www.fasteris.com/) performed additional small RNA sequencing on the Illumina HiSeq 2000 platform and following the manufacturer's recommended protocols.

Droplet Digital quantitative RT-PCR: 1.5 µg of DNase I-treated total RNA isolated from each sample was subjected to random-primed cDNA synthesis using Superscript III reverse transcriptase (Invitrogen) in 20 uL reactions, then diluted to 40 uL. TaqMan assays were assembled in 20 uL aliquots using 1 uL of cDNA. Reactions were combined with 70 uL of Droplet Generation Oil (Bio-Rad) in the QX100 Droplet Generator (Bio-Rad), and then partitioned into approximately 12000-15000 droplets, each ~1 nL. Forty cycles of standard PCR were performed on these emulsions, after which droplets were read as positive or negative for 6-FAM fluorescence on the QX100 Droplet Reader (Bio-Rad). Absolute concentrations were calculated based on the Poisson statistics, and gene expression was quantified relative to the *ACT2* constitutive control. TaqMan probes and primers used for droplet digital PCR are listed in Table S2.

Bioinformatic analyses: Illumina reads from non-stranded, polyA+ RNA-seq libraries were aligned to the *A. thaliana* TAIR10 annotated genome reference using Bowtie (V1.1.2) and Tophat (V1.1.2) (Langmead et al., 2009).

PolyA+ RNA-sequencing stats (perfect matches):

Library name	Mapped	Platform	Facility	Source
Col-0 WT1	38,981,185	Illumina GAIIx	CGB (IU)	this study
hda6-7	15,755,401	Illumina GAIIx	CGB (IU)	this study
pol IV (*nrpd1-3*)	20,953,165	Illumina GAIIx	CGB (IU)	this study
hda6 pol IV	33,450,389	Illumina GAIIx	CGB (IU)	this study
pol V (*nrpe1-11*)	36,353,829	Illumina GAIIx	CGB (IU)	this study
hda6 pol V	34,752,676	Illumina GAIIx	CGB (IU)	this study

Perfect (100%) matches were tallied at annotated genomic features. Transposable element (TE) expression by family (Figure 1A, 1B) was evaluated by counting family-specific reads, clustering normalized totals with R heatmap.2 and plotting with ggplot2 (Wickham, 2009). For all remaining polyA+ RNA analyses (Figures 1C, S1B, S1C), TAIR10 Representative Gene Models of types “mRNA” and “ncRNA” were considered as “Genes”, whereas coordinates for TAIR10 TEs were refined in Cufflinks using data from the *hda6 pol IV* mutant. Only TEs not overlapping “Genes” were considered. Differential polyA+ RNA expression was assessed with NOISeq (v1.1.5) using RPKM normalization, k=0.5 and q=0.88 settings (Tarazona et al., 2012), taking only uniquely-mapped reads into consideration. Significance (p-values) for differential expression in mutant samples were estimated using a normal distribution (pnorm function in R) with reference to the expected value in wild-type (Col-0). Threshold filters of log2(mutant/Col-0) > 2.0 and $p < 0.01$ were applied to NOISeq gene lists before Venn diagram generation.

For small RNA analyses, trimmed reads were aligned to the *A.thaliana* reference with Novoalign (v2.05.13; Novocraft).

Small RNA-sequencing stats (20-25 nt RNAs):

Library name	Mapped	Platform	Facility	Source
Col-0 WT1 rep1	4,457,015	Illumina GAIIx	CGB (IU)	this study
hda6-7	1,279,965	Illumina GAIIx	CGB (IU)	this study
pol IV (*nrpd1-3*)	2,568,399	Illumina GAIIx	CGB (IU)	this study
hda6 pol IV	1,358,721	Illumina GAIIx	CGB (IU)	this study
pol V (*nrpe1-11*)	1,231,055	Illumina GAIIx	CGB (IU)	this study
hda6 pol V	1,395,941	Illumina GAIIx	CGB (IU)	this study
Col-0 WT1 rep2	6,458,512	Illumina HiSeq	Fasteris SA	this study
hda6-6	6,012,373	Illumina HiSeq	Fasteris SA	this study
HDA6-F, hda6-6	7,383,450	Illumina HiSeq	Fasteris SA	this study
Col-0 (inf)	2,641,533	Illumina GA	SALK	Lister et al. 2008
met1-3 (inf)	1,512,796	Illumina GA	SALK	Lister et al. 2008

Perfectly matched, 20-25 nt small RNA inserts were analyzed using a combination of Perl, Python and R scripts to generate the RNA-seq profiles and small RNA size histograms (Figures

2A, 2C, 3A, 4A, 6B, 6C, 7A, S4). Average 24 nt small RNA density at each Gene was computed by dividing the sum of normalized base coverage in a given annotation interval by its total length. Log_2 density ratios (Col-0/*nrpd1*) and (Col-0/*hda6*) were approximated after adding pseudo-counts to the numerator and denominator, then plotted in R (Figure 4B). Chromosome-wide density plots (Figure 6A) were generated using the normalized abundance of 24-nt siRNAs in *de novo*-identified clusters (ShortStack, Axtell, 2013) for a 200-kb window stepped in 100-kb increments, and plotting density values distributed along each chromosome as heatmaps in ggplot2. For boxplot analyses, TAIR8 coordinates of siRNA clusters reported by (Law et al., 2013) were converted to corresponding TAIR10 positions, and small RNA reads aligned within these cluster boundaries were counted using ShortStack. Normalized, per-cluster counts were used as input for the R functions boxplot and wilcox.test to obtain Figures 6D, 6E, 7B, S7A and S7D. For profiling DNA methylation at loci divided by expression group (i.e., housekeeping, Group DL or Group E), locations of CG, CHG and CHH sites were computed based on TAIR10 genome annotations and hand annotation of small RNA-generating regions (e.g., those at *SDC*, *AtSN1*, *soloLTR* and *ERT* loci). The number of sites (m) with at least 10% methylation in wild-type Col-0 was extracted from data of (Stroud et al., 2013). The percentage of methylated sites was calculated (100*m/n) and the mean average taken across the entire expression group (Figure S1A).

IV. Supplemental References

Axtell, M.J. (2013). ShortStack: Comprehensive annotation and quantification of small RNA genes. RNA *19*, 740-751.

Kozomara, A., and Griffiths-Jones, S. (2011). miRBase: integrating microRNA annotation and deep-sequencing data. Nucleic Acids Res *39*, D152-157.

Langmead, B., Trapnell, C., Pop, M., and Salzberg, S.L. (2009). Ultrafast and memory-efficient alignment of short DNA sequences to the human genome. Genome biology *10*, R25.

Law, J.A., Du, J., Hale, C.J., Feng, S., Krajewski, K., Palanca, A.M., Strahl, B.D., Patel, D.J., and Jacobsen, S.E. (2013). Polymerase IV occupancy at RNA-directed DNA methylation sites requires SHH1. Nature.

Mortazavi, A., Williams, B.A., McCue, K., Schaeffer, L., and Wold, B. (2008). Mapping and quantifying mammalian transcriptomes by RNA-Seq. Nature methods *5*, 621-628.

Stroud, H., Greenberg, M.V., Feng, S., Bernatavichute, Y.V., and Jacobsen, S.E. (2013). Comprehensive analysis of silencing mutants reveals complex regulation of the Arabidopsis methylome. Cell *152*, 352-364.

Tarazona, S., Furio-Tari, P., Ferrer, A., and Conesa, A. (2012). NOISeq: Exploratory analysis and differential expression for RNA-seq data. *R package version 1.1.5.*

Wickham, H. (2009). ggplot2: elegant graphics for data analysis (New York: Springer).